Article

Not peer-reviewed version

Cost-Effective Carbon Dioxide Removal via CaO-based Mineralization with Concurrent Recovery of Value-Added Calcite Nanoparticles

Seungyeol Lee * and Gyujae You

Posted Date: 13 August 2025

doi: 10.20944/preprints202508.0957.v1

Keywords: CO_2 sequestration; calcite nanoparticles; X-ray diffraction; transmission electron microscopy; techno-economic analysis

 doi:10.20944/preprints202508.0957.v1

Article

Cost-Effective Carbon Dioxide Removal via CaO-Based Mineralization with Concurrent Recovery of Value-Added Calcite Nanoparticles

Seungyeol Lee [1,*] and Gyujae Yoo [2]

[1] Department of Earth and Environmental Sciences, Chungbuk National University, Cheongju 28644, Republic of Korea

[2] Bio Calcium Co., Ltd., Dong-myeon, Hwasun-gun, Jeollanam-do 58143, Republic of Korea

* Correspondence: slee2@cbnu.ac.kr

Abstract

The rapid increase in atmospheric CO_2 concentrations has intensified the demand for scalable, sustainable, and economically viable carbon sequestration technologies. This study presents a cost-effective calcium oxide (CaO)-based mineralization process that not only achieves efficient CO_2 removal but also enables the simultaneous recovery of high-purity calcite nanoparticles as value-added products. The process consists of hydrating CaO, followed by controlled carbonation under optimized CO_2 flow rates and temperature conditions, producing nanocrystalline calcite with an average particle size of approximately 100 nm. Comprehensive characterization using X-ray diffraction, transmission electron microscopy, and energy-dispersive X-ray spectroscopy confirmed a polycrystalline nanoparticle structure with exceptional chemical purity (99.9%) and rhombohedral morphology. A techno-economic analysis further revealed that integrating CO_2 sequestration with nanoparticle production can significantly enhance profitability, particularly when utilizing CaO-rich industrial residues such as steel slags or lime sludge as feedstock. This hybrid, multi-revenue approach—combining carbon credits, nanoparticle sales, and waste valorization—provides a scalable pathway aligned with circular economy principles, improving both environmental and economic performance. The findings highlight the potential of CaO-based mineralization to evolve from a carbon management solution into a platform for advanced materials manufacturing, thereby contributing to global decarbonization goals.

Keywords: CO_2 sequestration; calcite nanoparticles; X-ray diffraction; transmission electron microscopy; techno-economic analysis

1. Introduction

The continuous rise in atmospheric CO_2 concentrations has amplified the global demand for scalable, sustainable, and cost-effective carbon sequestration technologies. Among various strategies, mineralization-based carbon sinks are gaining recognition as practical and long-term solutions for mitigating climate change impacts [1]. From a geological perspective, mineral carbonation—where CO_2 reacts with calcium- or magnesium-rich silicate and ultramafic rocks to form stable carbonate minerals—offers one of the most permanent sequestration pathways, with storage stability over millions of years [2]. In addition, in-situ mineralization processes can be integrated with geothermal energy recovery, creating opportunities for co-benefits in both energy generation and carbon management [3]. Economic viability and operational efficiency remain decisive factors for global implementation of carbon capture systems and methods that immobilize CO_2 in geologically secure forms while producing valuable by-products—such as construction-grade carbonates—can substantially enhance their feasibility [4].

 doi:10.20944/preprints202508.0957.v1

Within mineral carbonation technologies, calcium oxide (CaO)-based mineralization has emerged as one of the most promising pathways for CO_2 sequestration, owing to its ability to permanently convert atmospheric or industrial CO_2 emissions into stable calcium carbonate minerals [5]. Unlike other capture techniques requiring costly storage infrastructure or energy-intensive regeneration cycles, CaO-based processes provide a direct, exothermic reaction pathway with strong thermodynamic favorability [5]. From a mineralogical standpoint, CaO carbonation proceeds through nucleation and growth of crystalline phases—predominantly calcite, along with aragonite and vaterite—whose stability and morphology depend on parameters such as temperature, CO_2 partial pressure, and the presence of aqueous phases [2]. The resulting carbonates exhibit high crystallographic stability, ensuring permanence on geological timescales [1]. Microstructural studies also reveal that the formation of nano- to micro-sized calcite crystals not only enhances CO_2 sequestration efficiency but also yields materials with functional properties suited for high-value industrial applications [6].

Recent research highlights the dual benefits of CaO-based mineralization: efficient CO_2 capture and simultaneous production of high-value by-products. These systems demonstrate rapid carbonation kinetics, high CO_2 uptake efficiency, and compatibility with industrial waste streams (e.g., slags, fly ash), making them well-suited for large-scale deployment [7]. Furthermore, there is increasing interest in optimizing carbonation conditions to selectively synthesize nano-sized calcite particles with high surface area, tunable morphology, and chemical stability. Such properties enable diverse applications in biomedicine (e.g., drug delivery, bone tissue engineering), polymer and paper industries, coatings, and environmental remediation [8–11]. At the nanoscale, calcite offers superior dispersion, mechanical integration, and reactivity in composite materials, reducing reliance on costly synthetic fillers and improving commercial competitiveness [6,12].

Integrating calcite nanoparticle recovery into CaO-based mineralization represents a paradigm shift from waste-focused sequestration toward resource-oriented valorization. This approach aligns with circular economy principles, transforming CO_2 from an emission challenge into a feedstock for sustainable material production [1,13]. Against this backdrop, the present study seeks to develop a cost-effective and scalable CaO-based CO_2 sequestration process that achieves both efficient carbon capture and recovery of high-purity calcite nanoparticles. Specifically, the research aims to: (1) Optimize carbonation parameters—such as temperature, CO_2 flow rate, and CaO particle size—to maximize CO_2 fixation efficiency; (2) Characterize the physicochemical properties of calcite nanoparticles, including morphology, crystallinity, and surface area; (3) Assess the economic and application potential of recovered nanoparticles in industrial sectors. By coupling CO_2 sequestration with nanomaterial synthesis, this study aims to propose a sustainable and economically viable pathway for carbon management that contributes to climate change mitigation while enabling circular resource utilization.

2. Materials and Methods

2.1. Process Description for CO_2 Mineralization and Byproduct Valorization

The proposed system for carbon dioxide removal and by-product valorization employs a multi-stage CaO-based mineralization process designed to maximize CO_2 capture efficiency while enabling the synthesis of high-value calcium carbonate nanoparticles. The methodology integrates a sequence of physical and chemical unit operations to optimize reaction kinetics, control particle morphology, and ensure consistent product quality (Figure 1).

 doi:10.20944/preprints202508.0957.v1

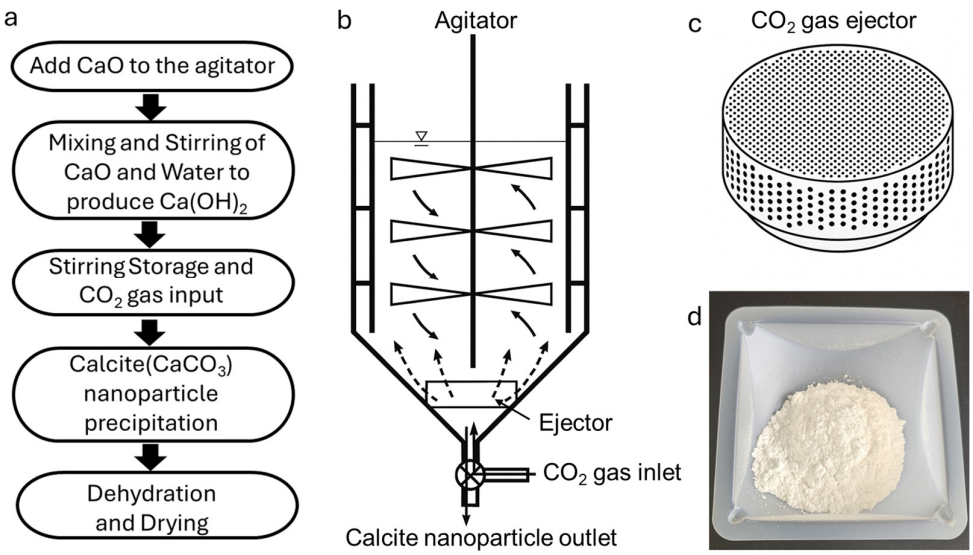

Figure 1. (a) Process flow diagram illustrating the CaO-based CO_2 mineralization system; (b) schematic illustration of the carbonation reactor assembly, (c) close-up view of the CO_2 ejector used to enhance gas–liquid mass transfer efficiency and ensure uniform dispersion of CO_2 within the slurry; (d) image of the final calcite nanoparticle product.

The process begins with the preparation of calcium oxide (CaO, quicklime), which may undergo preliminary crushing to achieve an optimal particle size distribution for rapid hydration and carbonation reactions. The prepared CaO is introduced into a mixing tank equipped with a mechanical agitator, where it is combined with water to form calcium hydroxide ($Ca(OH)_2$) slurry via an exothermic hydration reaction:

$$CaO + H_2O \rightarrow Ca(OH)_2 \quad (1)$$

The particle size and hydration conditions in this stage directly influence the surface area and reactivity of the resulting $Ca(OH)_2$. Following hydration, the slurry is transferred to a buffer tank for secondary agitation and pH stabilization. To facilitate the formation of uniform colloidal seed particles, an additive such as sodium glutamate, sugar, or a mixture is introduced at 0.1–2.0 parts by weight per 100 parts $Ca(OH)_2$. These additives act as crystal growth modifiers, influencing nucleation and controlling particle morphology at the nanoscale. This step also ensures completion of hydration and prepares the slurry for efficient CO_2 absorption. The conditioned slurry is pumped into a reaction chamber, where CO_2 gas is sparged through a gas ejector system. A controlled flow rate of 50–150 L/min per kg of $Ca(OH)_2$ promotes the formation of colloidal $CaCO_3$ seed particles with a cubic crystal habit and an average particle size of approximately 100 nm. Particle size and morphology can be adjusted by controlling the CO_2 flow rate and reaction time. The carbonation reaction proceeds as follows:

$$Ca(OH)_2 + CO_2 \rightarrow CaCO_3 + H_2O \quad (2)$$

Direct gas–liquid contact ensures high mass transfer rates and rapid mineralization, resulting in high conversion efficiency. The aqueous $CaCO_3$ slurry produced in the reactor is collected in a storage tank and can be used directly in liquid form. For applications requiring solid or semi-solid products, the slurry undergoes mechanical dewatering in a dehydrator to produce a gel-like paste. This paste is then dried—preferably using microwave-assisted drying to preserve particle morphology—resulting in granular solids. The dried material can be milled into a fine powder to meet the specifications of various industrial applications, such as polymer fillers, paper coatings, biomedical products, and advanced composite materials.

 doi:10.20944/preprints202508.0957.v1

2.2. Characterization

Characterization of the synthesized nano-calcium carbonate was performed at the Mineralogy and Mineral Resources Laboratory, Department of Earth and Environmental Sciences, Chungbuk National University (CBNU), and the CBNU Central Laboratory for Instrumentation and Research. Powder X-ray diffraction (XRD) analysis was carried out using a Rigaku Miniflex 600 powder X-ray diffractometer equipped with a Cu Kα radiation source (λ = 1.5406 Å) operated at 40 kV and 15 mA. Data were collected over the 2θ range of 5–80°, with a step size of 0.1° and a scan rate of 3°·min^{-1} to ensure adequate peak resolution. Prior to measurement, the instrument was calibrated using a standard silicon reference material to correct systematic errors.

Morphological observations and elemental analyses were conducted using a JEOL JSM-IT510 scanning electron microscope (SEM) operated at an accelerating voltage of 10–15 kV, under high-vacuum mode, and equipped with an Oxford Instruments energy-dispersive X-ray spectroscopy (EDS) system for qualitative and semi-quantitative elemental analysis. High-resolution imaging and structural analysis were conducted using a spherical aberration (Cs)-corrected transmission electron microscope (JEM-ARM200F, NEOARM; JEOL Ltd., Japan) operated at an accelerating voltage of 200 kV. Lattice-resolved images and Fast Fourier Transform (FFT) patterns were obtained to investigate the crystal structure at the nanoscale. TEM specimens were prepared by dispersing the powder sample in ethanol, followed by ultrasonication for 10 min to prevent particle agglomeration. A drop of the suspension was then deposited onto copper carbon lacey grids and dried under ambient conditions prior to analysis.

3. Results

3.1. Powder X-Ray Diffraction

XRD analysis was conducted to examine the phase composition, crystallinity, and structural characteristics of the synthesized calcium carbonate byproduct, with the objective of confirming the formation of the calcite polymorph. The diffraction pattern exhibited a series of sharp and intense peaks, characteristic of a well-ordered crystalline material (Figure 2). Peak positions and relative intensities showed complete agreement with reference data [14] for rhombohedral calcite (space group *R*3*c*). Prominent reflections, including the (10$\bar{2}$), (104), (110), (1$\bar{2}$3), and (202) planes, were consistent with the standard pattern, indicating the exclusive presence of calcite. No diffraction signals attributable to alternative $CaCO_3$ polymorphs, such as aragonite or vaterite, were detected, confirming the high phase purity of the synthesized product. The nanocrystalline nature of the calcite was further confirmed by estimating the average crystallite size using the Scherrer equation, applied to the full width at half maximum of the dominant reflections. The calculated crystallite size was approximately 86 nm, indicating that the product exists in the nanometer size range. The narrow and symmetric diffraction peaks also suggest minimal lattice strain and a uniform crystallite distribution. These results demonstrate that the synthesis process successfully produced a phase-pure, highly crystalline, nanocrystalline calcite without detectable secondary calcium carbonate polymorphs.

 doi:10.20944/preprints202508.0957.v1

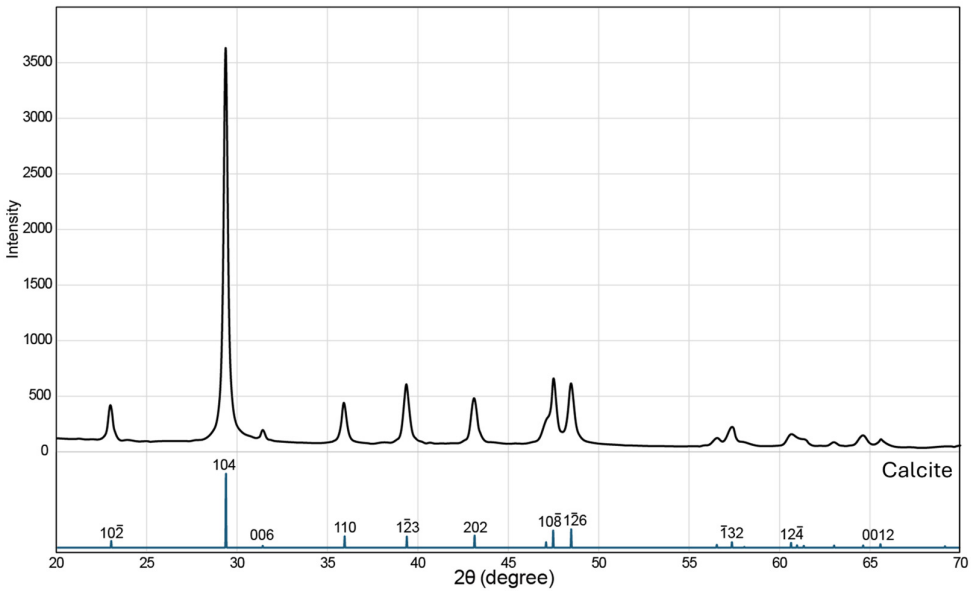

Figure 2. Powder XRD pattern of the synthesized calcite nanoparticles. All major diffraction peaks correspond to rhombohedral calcite matching the calcite structure [14]. The absence of peaks from other $CaCO_3$ polymorphs such as aragonite or vaterite confirms phase purity. The sharp and symmetric peak profiles indicate high crystallinity, while the average crystallite size, calculated using the Scherrer equation from the (104) reflection, is ~86 nm.

3.2. Transmission Electron Microscopy

To elucidate the morphology and size characteristics of the synthesized byproduct, a multi-modal electron microscopy approach was employed. Initial SEM imaging was insufficient to resolve individual primary particles due to nanoscale resolution limitations. Consequently, TEM was utilized to obtain high-resolution images, which revealed discrete nanoparticles exhibiting a well-defined rhombohedral habit (Figure 3a,b). This morphology is consistent with the rhombohedral crystal structure of calcite confirmed by XRD analysis. A statistical size analysis was conducted by measuring 536 nanoparticles from TEM micrographs (Figure 3c). The particle size distribution, determined using a 10 nm bin width, ranged from 60 to 200 nm and exhibited a unimodal but positively skewed profile. The majority of particles fell within the 70–110 nm range, with a mean size of approximately 105 nm. The narrow, dominant peak indicates that the reaction conditions promoted stable, well-controlled nucleation and growth, while the extended right-hand tail suggests the presence of a minor population of larger particles, likely formed via partial irreversible agglomeration or Ostwald ripening. Such size distribution characteristics are critical, as particle size and monodispersity directly influence the functional performance of nanomaterials in applications such as catalysis, composite reinforcement, and optical systems. TEM coupled with EDS confirmed the high chemical purity of the nanoparticles, detecting only calcium, carbon, and oxygen, with no other elemental impurities(Figure 3d). The estimated purity of 99.9% is attributed to the use of high-grade CaO precursors in the synthesis. This compositional purity is a key requirement for high-value applications.

 doi:10.20944/preprints202508.0957.v1

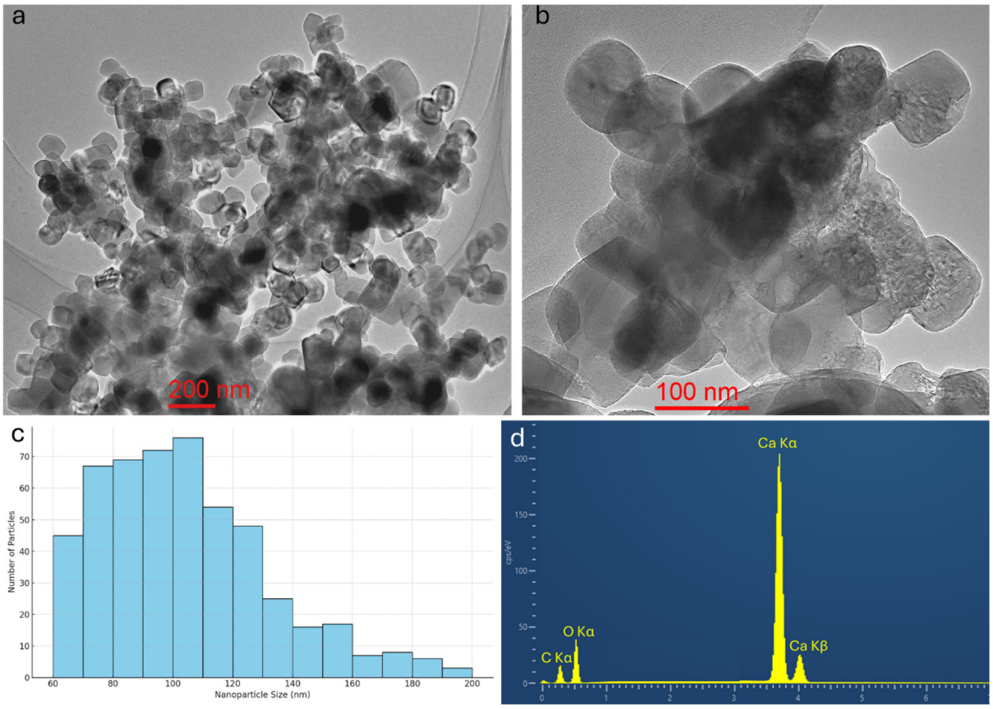

Figure 3. (a–b) Representative bright-field TEM images of the synthesized calcite nanoparticles, clearly exhibiting discrete particles with well-defined rhombohedral morphology; (c) particle size distribution histogram derived from measurements of 536 individual nanoparticles, showing a unimodal but positively skewed profile with the majority of particles in the 70–110 nm range; (d) EDS spectrum of the nanoparticles, revealing only calcium, carbon, and oxygen peaks, confirming high chemical purity with no detectable elemental impurities.

High-resolution TEM (HRTEM) imaging revealed well-defined lattice fringes, indicative of high local crystallinity (Figure 4). FFT analysis of the HRTEM images yielded diffraction spot patterns that were indexed to the rhombohedral calcite structure, showing excellent agreement with simulated electron diffraction patterns along major crystallographic orientations, including the b-axis and c-axis. Notably, HRTEM observations demonstrated that, particularly along the c-axis, the calcium polyhedra at the boundaries of the a- and b-axes are in contact with a distinct lattice mismatch (Figure 5). This interfacial misfit is clearly manifested in the corresponding FFT patterns. Closer inspection revealed that the nanoparticles are polycrystalline aggregates composed of multiple nanodomains with varied orientations, rather than single crystals. While each domain is a coherent crystalline unit, the misorientation between domains limits long-range order. The combination of preserved rhombohedral morphology, surface roughness, visible grain boundaries, and internal nanodomain arrangement suggests a non-classical growth pathway, likely via oriented attachment of primary nanocrystals.

 doi:10.20944/preprints202508.0957.v1

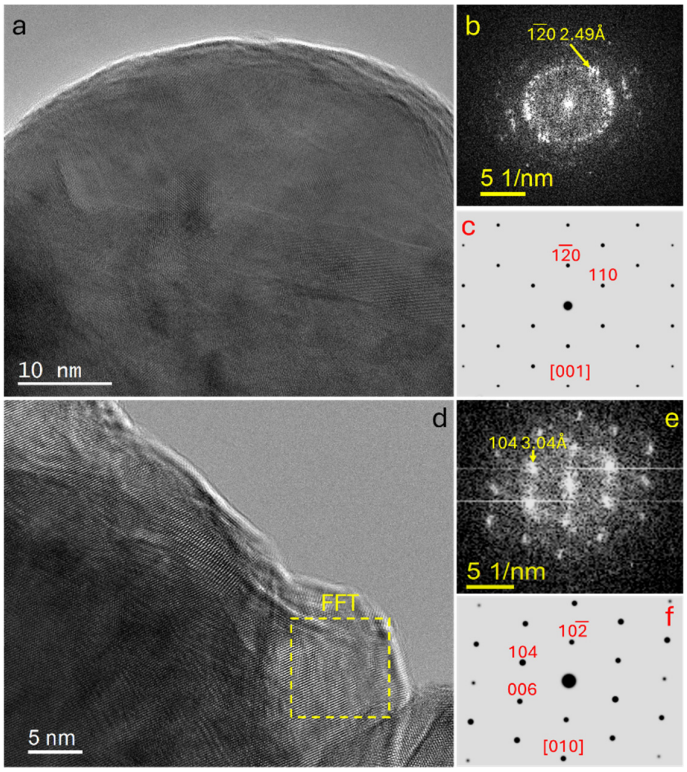

Figure 4. (a) HRTEM image of an individual nanocrystalline grain within a calcite nanoparticle, showing well-resolved lattice fringes; (b) corresponding FFT pattern of the entire grain; (c) simulated electron diffraction pattern of calcite viewed along the [001]-zone axis for comparison; (d) HRTEM image of another nanocrystalline domain within a different particle; (e) selected-area FFT pattern (yellow dash) extracted from the domain in (d); (f) simulated calcite electron diffraction pattern corresponding to the crystallographic orientation observed in (e).

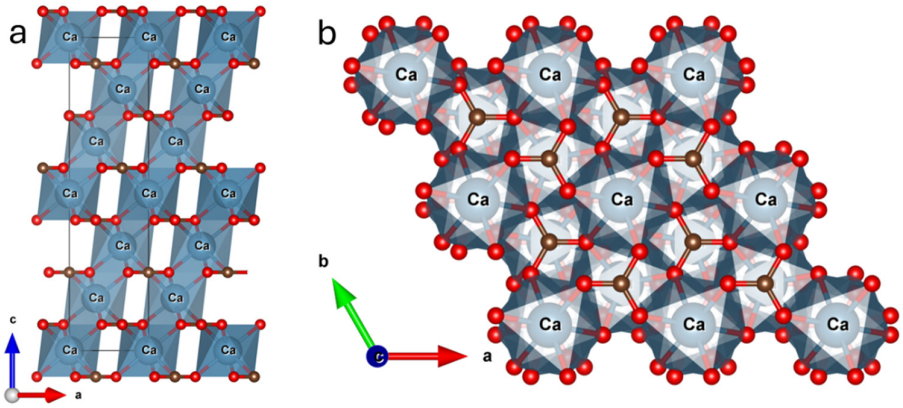

Figure 5. Illustration of the calcite crystal structure viewed along (a) the b-axis and (b) the c-axis. Brown spheres represent carbon atoms, and red spheres represent oxygen atoms, highlighting the arrangement of carbonate groups within the rhombohedral lattice.

4. Discussion

4.1. Process Control for Calcite Nanoparticle Formation

A central challenge—and a decisive success factor—in CaO-based CO_2 mineralization lies in achieving simultaneous optimization of carbon fixation efficiency and nanoparticle quality control [2]. The physicochemical attributes of the final calcite nanoparticles—particularly size, crystallinity, morphology, and purity—are highly sensitive to process parameters, all of which must be precisely

 doi:10.20944/preprints202508.0957.v1

tuned to deliver products suited for high-value applications [6,16]. From an economic perspective, the rationale for producing calcite nanoparticles rather than micron-scale calcite is compelling [16,17]. Micron-sized particles have limited market value and constrained applicability in advanced functional materials [18]. In contrast, nanoscale calcite offers markedly higher surface area, enhanced reactivity, and tunable optical properties, making it highly attractive for applications such as biomedical fillers, advanced composites, and photonic materials. By implementing well-designed process control strategies, it is possible not only to consistently produce nanoparticles but also to selectively tailor particle size distributions—enabling the targeted manufacture of specific size fractions to match diverse industrial requirements and thereby improving commercial viability.

Among the most critical operational parameters are reaction temperature, CO_2 gas injection rate, pH control, and CaO precursor characteristics (particle size, surface area, and purity). Elevated temperatures (>50 °C) can accelerate carbonation by enhancing reaction kinetics and increasing CO_2 solubility in the aqueous phase[19]. However, such thermal conditions also promote uncontrolled crystal growth, leading to particle coarsening and a broader size distribution—undesirable for applications requiring monodispersity [20,21]. The CO_2 injection rate governs gas–liquid mass transfer efficiency and local supersaturation. As previous reported, high flow rates can significantly increase nucleation rates but may also cause localized pH gradients and rapid precipitation, resulting in amorphous or poorly crystalline phases and particle agglomeration. Excessively high injection rates can overwhelm the system's buffering capacity, further amplifying variability in particle size and morphology [18–20]

pH control emerges as an equally important, yet often underemphasized, factor in nanoparticle synthesis. The saturation state of carbonate species and the stability of intermediate phases (e.g., amorphous calcium carbonate) are pH-dependent, directly influencing nucleation kinetics, crystal habit, and final particle size [22]. Maintaining a controlled pH window during carbonation—particularly in the range that stabilizes critical nuclei while suppressing rapid, uncontrolled precipitation—can yield narrower size distributions and higher monodispersity [23]. Conversely, uncontrolled pH fluctuations can trigger premature aggregation or phase transformations, undermining particle uniformity and functional performance [21,22].

The CaO precursor also plays a decisive role. Nanoscale CaO particles provide abundant reactive sites but are prone to early-stage agglomeration during hydration and carbonation, which can reduce dispersion quality [24,25]. Impurities or secondary mineral phases in the precursor can disrupt controlled nucleation and growth pathways. High-resolution TEM observations reveal that the synthesized calcite nanoparticles exhibit a polycrystalline architecture, consistent with a non-classical crystallization pathway. Rather than forming solely through stepwise monomer addition, the particles appear to develop via oriented attachment (OA) of primary nanocrystalline domains, followed by Ostwald ripening—where larger, more stable particles grow at the expense of smaller ones. These mechanisms, widely recognized in biomineralization and synthetic systems, are governed by the interplay of kinetic and thermodynamic factors that dictate phase selection, particle aggregation, and morphological evolution [26,27]

In prolonged reactions or under sustained CO_2 saturation, OA-driven growth and secondary ripening are more pronounced, often producing irregular aggregates and broader size distributions [27]. Thus, integrated control—combining CO_2 dosing profiles, temperature management, pH stabilization, and the use of crystal growth modifiers—is essential to suppress undesirable growth pathways. Additives such as sugar derivatives or amino acids can selectively inhibit particle fusion and regulate crystal habit, further enhancing monodispersity and functional performance. The economic imperative for producing calcite nanoparticles, combined with the ability to precisely tune particle size via temperature, CO_2 flow, pH, and precursor engineering, underscores the importance of mastering both classical and non-classical growth mechanisms (Table 1). Such process mastery not only enhances product performance in high-end applications but also enables the creation of market-differentiated nanoparticle products with optimized size, purity, and functionality, thereby bridging carbon capture with advanced materials manufacturing [24].

 doi:10.20944/preprints202508.0957.v1

Table 1. This is a table. Tables should be placed in the main text near to the first time they are cited.

Parameter	Primary Influence	Optimal Condition	Potential Negative Effects
Reaction Temperature	Controls carbonation kinetics & CO_2 solubility; affects nucleation rate	30-50 °C -> balanced kinetics & controlled crystal growth	High T -> uncontrolled Growth/coarsening; Low T-slow reaction
CO_2 Injection Rate	Governs gas-liquid mass transfer & local supersaturation	Moderate flow -> efficient nucleation without uncontrolled precipitation	High rate -> pH gradients, amorphous phases, agglomeration
pH Control	Regulates carbonate speciation & stability of intermediate phases	pH 8.5-9.5 -> stabilizes nuclei & controls growth	Large pH swings -> premature aggregation, phase transformation
CaO Precursor Characteristics	Determines reactive surface area & nucleation sites	Fine particle size, high surface area, high purity	Impurities -> disrupt nucleation; ultra-fine -> early agglomeration

4.2. Characteristics and High-Value Application Potential of Synthesized Calcite Nanoparticles

The calcite nanoparticles synthesized in this process—averaging approximately 100 nm in size—are not merely a medium for CO_2 storage, but constitute a high-value product in their own right. At this scale, calcite exhibits physicochemical characteristics that fundamentally distinguish it from bulk calcium carbonate, including a high specific surface area, uniform rhombohedral morphology, and intrinsic biocompatibility [28]. These attributes confer enhanced reactivity, excellent dispersibility, and superior interfacial performance, making nanoscale calcite highly sought after in a range of high-performance industrial and biomedical applications [29,30].

In the biomedical sector, ~100 nm calcite particles have been investigated as core materials for drug delivery, gene transfection, and bone tissue engineering [9,11,31]. Their pH-responsive solubility in acidic microenvironments—such as those present in tumor tissues—enables controlled and targeted therapeutic release [32]. Furthermore, their crystallographic and chemical similarity to natural bone minerals promotes osteogenic activity and biointegration when incorporated into orthopedic scaffolds [9]. In the polymer and composite industries, nano-calcite serves as a highly efficient functional filler, significantly improving tensile strength, impact resistance, and thermal stability [6,17]. Due to their nanoscale dimensions and superior dispersion, these particles can achieve equivalent or greater performance enhancements at much lower loadings compared to conventional micron-sized fillers. This yields a favorable cost-to-performance ratio, making them advantageous for demanding sectors such as automotive components, high-barrier packaging films, and biodegradable plastics [6].

The 100 nm calcite nanoparticles produced in this study—characterized by confirmed phase purity, high crystallinity, and minimal agglomeration—align closely with the stringent specifications of these high-value markets. Moreover, the process developed here offers flexibility in tuning particle size and morphology to match specific market demands. By adjusting process parameters such as temperature, CO_2 injection rate, pH, and additive type, it is feasible to produce tailored morphologies, including whisker-shaped nano-calcite (Table 1). Such whisker-type particles have already been demonstrated as high-performance fillers in specialty paper manufacturing, enhancing mechanical strength, opacity, and printability [33]. This adaptability indicates that the present method can be extended beyond rhombohedral nanoparticles to produce application-specific morphologies, further broadening its industrial applicability and market potential [31,33].

4.3. Integrated Techno-Economic Assessment: Building a Multi-Revenue Model

Theoretically, 1 kg of CaO can capture up to 784.77 g of CO_2, corresponding to a mass efficiency of approximately 78.5%, underscoring its strong sequestration potential [24]. However, when assessed solely on the basis of carbon credit revenues, the economic feasibility remains limited.

 doi:10.20944/preprints202508.0957.v1

Industrial-grade CaO costs approximately \$0.15 kg^{-1}, while the average market value of CO_2 credits—depending on regional pricing—translates to only \$0.039–\$0.078 kg^{-1} of CaO reacted [34]. This disparity indicates that a carbon-credit-only model is insufficient to achieve profitability, especially when operational costs for CO_2 capture, slurry preparation, and post-processing are taken into account (Figure 6).

A viable solution lies in the co-recovery and commercialization of high-value calcite nanoparticles as a parallel revenue stream. Conventional bulk $CaCO_3$ sells for only \$30–\$80 t^{-1}, whereas high-purity nano-calcite—particularly in the 50–200 nm range—can command \$300 to >\$1,000 t^{-1}, depending on morphological uniformity, surface properties, and application sector [34,35]. Given that 1 kg of CaO yields approximately 1.78 kg of $CaCO_3$, and assuming 60–70% recovery as nano-grade material, revenues from material sales alone could surpass raw material and processing costs by a significant margin—effectively transforming the process from a cost center into a net revenue generator.

Further economic and environmental benefits can be realized by substituting commercial CaO with CaO-rich industrial residues, such as lime sludge from water treatment plants, demolished concrete fines, or steelmaking slags [13,18]. This substitution not only reduces feedstock costs to near zero but also eliminates the environmental burden of quarrying and calcining limestone, while diverting alkaline wastes from landfills—thereby achieving waste valorization and aligning with circular economy principles. Moreover, many waste-derived CaO sources exhibit high reactivity due to their fine particle size and elevated surface area, potentially enhancing carbonation kinetics [36].

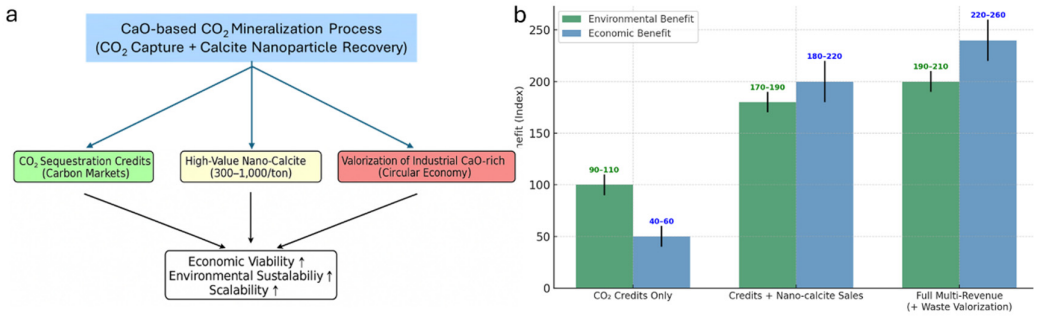

Figure 6. (a) Schematic representation of the integrated multi-revenue model for CaO-based CO_2 mineralization, illustrating three synergistic revenue streams. The integration of these streams enhances economic viability, environmental sustainability, and scalability. (b) Comparative assessment of environmental (green bars) and economic (blue bars) benefits for different revenue models, expressed as relative benefit indices with range values. Models include CO_2 credits only, credits combined with nano-calcite sales, and the full multi-revenue approach incorporating waste valorization. Error bars indicate estimated benefit variability based on market and operational parameters.

From a techno-economic standpoint (Figure 6), integrating these strategies yields a multi-revenue business model with three primary income streams: (1)CO_2 sequestration credits — monetizing verified emission reductions; (2) Production and sale of high-margin calcite nanoparticles for premium markets in biomedicine, polymers, and coatings; (3) Valorization of CaO/$Ca(OH)_2$-bearing industrial residues — generating added value from materials that would otherwise be disposal liabilities. This integrated approach not only strengthens process economics but also enhances the life-cycle sustainability profile of CaO-based mineralization technologies [19]. By coupling carbon mitigation with advanced material manufacturing, the system achieves higher returns on investment, greater scalability, and stronger alignment with global decarbonization and resource efficiency objectives [36].

 doi:10.20944/preprints202508.0957.v1

5. Conclusions

This study demonstrates that CaO-based CO_2 mineralization, when integrated with the concurrent recovery of high-purity calcite nanoparticles, can transform from a conventional carbon capture strategy into a value-generating, resource-oriented industrial process. Under optimized reaction conditions, the process yielded calcite nanoparticles with an average size of ~100 nm, high crystallinity, phase purity, and minimal agglomeration—properties that align with the stringent specifications required in advanced applications such as biomedicine, polymer composites, and specialty coatings. From an economic perspective, a carbon-credit-only model is insufficient to offset raw material and processing costs. In contrast, incorporating the sale of high-margin nano-calcite—priced significantly above bulk calcium carbonate—enables the process to achieve profitability. Additional gains can be realized by replacing commercial CaO with CaO-rich industrial residues, thereby lowering raw material costs, reducing waste disposal burdens, and advancing circular economy objectives. Techno-economic analysis confirms that a multi-revenue model—combining (1) CO_2 sequestration credits, (2) high-value nano-calcite sales, and (3) valorization of CaO-bearing industrial residues—substantially improves both profitability and sustainability. This integrated approach not only addresses the urgent need for scalable, cost-effective carbon removal, but also contributes to the production of next-generation functional materials, positioning CaO-based mineralization as a strategic platform technology for climate change mitigation and sustainable manufacturing.

Future work should focus on refining process control strategies to tailor particle size, morphology, and surface chemistry to meet specific market requirements, as well as conduct long-term pilot-scale demonstrations to validate economic performance under real industrial conditions. With these advancements, CaO-based CO_2 mineralization has the potential to become a pivotal component of global decarbonization strategies, delivering tangible economic, environmental, and technological co-benefits.

Author Contributions: Conceptualization, S.L.; methodology, S.L. and G.Y.; formal analysis, S.L. and G.Y; investigation, S.L. resources, S.L. and G.Y.; data curation, S.L.; writing—original draft preparation, S.L.; writing—review and editing, S.L.; visualization, S.L.; supervision, S.L.; funding acquisition, S.L. All authors have read and agreed to the published version of the manuscript.

Funding: This work was supported by the National Research Foundation of Korea(NRF) grant funded by the Korea government(MSIT) (No. RS-2024-00342773). This research was supported by Global - Learning & Academic research institution for Master's·PhD students, and Postdocs(LAMP) Program of the National Research Foundation of Korea(NRF) grant funded by the Ministry of Education(No. RS-2024-00445180).

Institutional Review Board Statement: Not applicable.

Informed Consent Statement: Not applicable.

Data Availability Statement: The data used in this study can be requested from the authors.

Conflicts of Interest: The authors declare no conflicts of interest.

References

1. Power, I.M.; Harrison, A.L.; Dipple, G.M.; Wilson, S.; Kelemen, P.B.; Hitch, M.; Southam, G. Carbon Mineralization: From Natural Analogues to Engineered Systems. *Reviews in Mineralogy and Geochemistry* **2013**, *77*, 305–360, doi:10.2138/rmg.2013.77.9.
2. Kelemen, P.; Benson, S.M.; Pilorgé, H.; Psarras, P.; Wilcox, J. An Overview of the Status and Challenges of CO2 Storage in Minerals and Geological Formations. *Front. Clim.* **2019**, *1*, doi:10.3389/fclim.2019.00009.
3. Wu, Y.; Li, P. The Potential of Coupled Carbon Storage and Geothermal Extraction in a CO2-Enhanced Geothermal System: A Review. *Geotherm Energy* **2020**, *8*, 19, doi:10.1186/s40517-020-00173-w.

 doi:10.20944/preprints202508.0957.v1

4. Menefee, A.H.; Schwartz, B.A. Quantifying the Value of Geologic Carbon Mineralization for Project Risk Management in Carbon Capture and Removal Pathways. *Energy Fuels* **2024**, *38*, 5365–5373, doi:10.1021/acs.energyfuels.4c00138.
5. Romanov, V.; Soong, Y.; Carney, C.; Rush, G.E.; Nielsen, B.; O'Connor, W. Mineralization of Carbon Dioxide: A Literature Review. *ChemBioEng Reviews* **2015**, *2*, 231–256, doi:10.1002/cben.201500002.
6. Niu, Y.-Q.; Liu, J.-H.; Aymonier, C.; Fermani, S.; Kralj, D.; Falini, G.; Zhou, C.-H. Calcium Carbonate: Controlled Synthesis, Surface Functionalization, and Nanostructured Materials. **2022**, doi:10.1039/D1CS00519G.
7. Luo, Y.; He, D. Research Status and Future Challenge for CO2 Sequestration by Mineral Carbonation Strategy Using Iron and Steel Slag. *Environ Sci Pollut Res* **2021**, *28*, 49383–49409, doi:10.1007/s11356-021-15254-x.
8. Barhoum, A.; Rahier, H.; Abou-Zaied, R.E.; Rehan, M.; Dufour, T.; Hill, G.; Dufresne, A. Effect of Cationic and Anionic Surfactants on the Application of Calcium Carbonate Nanoparticles in Paper Coating. *ACS Appl. Mater. Interfaces* **2014**, *6*, 2734–2744, doi:10.1021/am405278j.
9. Zhao, P.; Tian, Y.; You, J.; Hu, X.; Liu, Y. Recent Advances of Calcium Carbonate Nanoparticles for Biomedical Applications. *Bioengineering* **2022**, *9*, 691, doi:10.3390/bioengineering9110691.
10. Yadav, V.K.; Yadav, K.K.; Cabral-Pinto, M.M.S.; Choudhary, N.; Gnanamoorthy, G.; Tirth, V.; Prasad, S.; Khan, A.H.; Islam, S.; Khan, N.A. The Processing of Calcium Rich Agricultural and Industrial Waste for Recovery of Calcium Carbonate and Calcium Oxide and Their Application for Environmental Cleanup: A Review. *Applied Sciences* **2021**, *11*, 4212, doi:10.3390/app11094212.
11. Maleki Dizaj, S.; Barzegar-Jalali, M.; Zarrintan, M.H.; Adibkia, K.; Lotfipour, F. Calcium Carbonate Nanoparticles as Cancer Drug Delivery System. *Expert Opinion on Drug Delivery* **2015**, *12*, 1649–1660, doi:10.1517/17425247.2015.1049530.
12. Thenepalli, T.; Jun, A.Y.; Han, C.; Ramakrishna, C.; Ahn, J.W. A Strategy of Precipitated Calcium Carbonate (CaCO3) Fillers for Enhancing the Mechanical Properties of Polypropylene Polymers. *Korean J. Chem. Eng.* **2015**, *32*, 1009–1022, doi:10.1007/s11814-015-0057-3.
13. Li, W.; Huang, Y.; Wang, T.; Fang, M.; Li, Y. Preparation of Calcium Carbonate Nanoparticles from Waste Carbide Slag Based on CO2 Mineralization. *Journal of Cleaner Production* **2022**, *363*, 132463, doi:10.1016/j.jclepro.2022.132463.
14. Lee, S.; Xu, H. Using Complementary Methods of Synchrotron Radiation Powder Diffraction and Pair Distribution Function to Refine Crystal Structures with High Quality Parameters—A Review. *Minerals* **2020**, *10*, 124, doi:10.3390/min10020124.
15. Markgraf, S.A.; Reeder, R.J. High-Temperature Structure Refinements of Calcite and Magnesite. *American Mineralogist* **1985**, *70*, 590–600.
16. Duffy, D.M. Coherent Nanoparticles in Calcite. *Science* **2017**, *358*, 1254–1255, doi:10.1126/science.aaq0111.
17. Biradar, S.; Ravichandran, P.; Gopikrishnan, R.; Goornavar, V.; Hall, J.C.; Ramesh, V.; Baluchamy, S.; Jeffers, R.B.; Ramesh, G.T. Calcium Carbonate Nanoparticles: Synthesis,Characterization and Biocompatibility. *Journal of Nanoscience and Nanotechnology* **2011**, *11*, 6868–6874, doi:10.1166/jnn.2011.4251.
18. Lee, J.; Ryu, K.H.; Ha, H.Y.; Jung, K.-D.; Lee, J.H. Techno-Economic and Environmental Evaluation of Nano Calcium Carbonate Production Utilizing the Steel Slag. *Journal of CO2 Utilization* **2020**, *37*, 113–121, doi:10.1016/j.jcou.2019.12.005.
19. Jiang, L.; Cheng, L.; Zhang, Y.; Liu, G.; Sun, J. A Review on CO2 Sequestration via Mineralization of Coal Fly Ash. *Energies* **2023**, *16*, 6241, doi:10.3390/en16176241.
20. Lee, A.Y.; Erdemir, D.; Myerson, A.S. Crystals and Crystal Growth. In *Handbook of Industrial Crystallization*; Lee, A.Y., Myerson, A.S., Erdemir, D., Eds.; Cambridge University Press: Cambridge, 2019; pp. 32–75 ISBN 978-0-521-19618-5.
21. Vinoba, M.; Bhagiyalakshmi, M.; Choi, S.Y.; Park, K.T.; Kim, H.J.; Jeong, S.K. Harvesting CaCO3 Polymorphs from In Situ CO2 Capture Process. *J. Phys. Chem. C* **2014**, *118*, 17556–17566, doi:10.1021/jp503448y.

 doi:10.20944/preprints202508.0957.v1

22. Bots, P.; Benning, L.G.; Rodriguez-Blanco, J.-D.; Roncal-Herrero, T.; Shaw, S. Mechanistic Insights into the Crystallization of Amorphous Calcium Carbonate (ACC). *Crystal Growth & Design* **2012**, *12*, 3806–3814, doi:10.1021/cg300676b.
23. Diego Rodriguez-Blanco, J.; Shaw, S.; G. Benning, L. The Kinetics and Mechanisms of Amorphous Calcium Carbonate (ACC) Crystallization to Calcite , via Vaterite. **2011**, doi:10.1039/C0NR00589D.
24. Wang, N.; Feng, Y.; Guo, X.; van Duin, A.C.T. Insights into the Role of H2O in the Carbonation of CaO Nanoparticle with CO2. *J. Phys. Chem. C* **2018**, *122*, 21401–21410, doi:10.1021/acs.jpcc.8b05517.
25. Álvarez Criado, Y.; Alonso, M.; Abanades, J.C. Composite Material for Thermochemical Energy Storage Using CaO/Ca(OH)2. *Ind. Eng. Chem. Res.* **2015**, *54*, 9314–9327, doi:10.1021/acs.iecr.5b02688.
26. De Yoreo, J.J.; Gilbert, P.U.P.A.; Sommerdijk, N.A.J.M.; Penn, R.L.; Whitelam, S.; Joester, D.; Zhang, H.; Rimer, J.D.; Navrotsky, A.; Banfield, J.F.; et al. Crystallization by Particle Attachment in Synthetic, Biogenic, and Geologic Environments. *Science* **2015**, *349*, aaa6760, doi:10.1126/science.aaa6760.
27. Li, D.; Nielsen, M.H.; Lee, J.R.I.; Frandsen, C.; Banfield, J.F.; De Yoreo, J.J. Direction-Specific Interactions Control Crystal Growth by Oriented Attachment. *Science* **2012**, *336*, 1014–1018, doi:10.1126/science.1219643.
28. Chang, R.; Kim, S.; Lee, S.; Choi, S.; Kim, M.; Park, Y. Calcium Carbonate Precipitation for CO2 Storage and Utilization: A Review of the Carbonate Crystallization and Polymorphism. *Front. Energy Res.* **2017**, *5*, doi:10.3389/fenrg.2017.00017.
29. Meldrum, F.C.; Cölfen, H. Controlling Mineral Morphologies and Structures in Biological and Synthetic Systems. *Chem. Rev.* **2008**, *108*, 4332–4432, doi:10.1021/cr8002856.
30. Lee, S.; Xu, H. Size-Dependent Phase Map and Phase Transformation Kinetics for Nanometric Iron(III) Oxides ($\gamma \rightarrow \varepsilon \rightarrow \alpha$ Pathway). *J. Phys. Chem. C* **2016**, *120*, 13316–13322, doi:10.1021/acs.jpcc.6b05287.
31. Ranjan, R.; Narnaware, S.D.; Patil, N.V. A Novel Technique for Synthesis of Calcium Carbonate Nanoparticles. *Natl. Acad. Sci. Lett.* **2018**, *41*, 403–406, doi:10.1007/s40009-018-0704-4.
32. Lee, S.; Xu, H. The Crystal Structure and Gibbs Free Energy of Formation of Chukanovite as an Oxidation Product of Carbon Steel in Human Liver. *Chemical Geology* **2018**, *488*, 180–188, doi:10.1016/j.chemgeo.2018.04.033.
33. Ulusoy, U. A Review of Particle Shape Effects on Material Properties for Various Engineering Applications: From Macro to Nanoscale. *Minerals* **2023**, *13*, 91, doi:10.3390/min13010091.
34. Agnolucci, P.; Fischer, C.; Heine, D.; Montes de Oca Leon, M.; Pryor, J.; Patroni, K.; Hallegatte, S. Measuring Total Carbon Pricing. *World Bank Res Obs* **2024**, *39*, 227–258, doi:10.1093/wbro/lkad009.
35. Al-Abdulqader, K.S.; Ibrahim, A.-J.; Ong, J.; Khalifa, A.A. Does Carbon Pricing Matter? Evidence from a Global Sample. *Energies* **2025**, *18*, 1030, doi:10.3390/en18051030.
36. Baena-Moreno, F.M.; Rodríguez-Galán, M.; Vega, F.; Alonso-Fariñas, B.; Vilches Arenas, L.F.; Navarrete, B. Carbon Capture and Utilization Technologies: A Literature Review and Recent Advances. *Energy Sources, Part A: Recovery, Utilization, and Environmental Effects* **2019**, *41*, 1403–1433, doi:10.1080/15567036.2018.1548518.